Rock Mech. Rock Engng. (2004) 37 (3), 193–212
DOI 10.1007/s00603-003-0006-z

Rock Mechanics and Rock Engineering
Printed in Austria

Composite Element Model of the Fully Grouted Rock Bolt

By

S.-H. Chen[1], **S. Qiang**[1], **S.-F. Chen**[1], and **P. Egger**[2]

[1] Department of Hydroelectrical Engineering, Wuhan University, Wuhan, P.R. China
[2] Swiss Federal Institute of Technology, Lausanne, Switzerland

Received November 20, 2002; accepted May 19, 2003
Published online August 18, 2003

Summary

The three dimensional elasto-viscoplastic composite element method is formulated in this paper for rock masses reinforced by a fully-grouted bolt. If a bolt segment penetrates a finite element representing the rock mass, then a composite element is formed including five sub-elements corresponding to the rock material, the grout material, the bolt material, the rock-grout interface and the bolt-grout interface. The displacements in each sub-element are interpolated from the corresponding nodal displacements of the composite element. By the virtual work principle the governing equation for the solution of the nodal displacements can be formulated. The elasto-viscoplastic characteristics of the materials are considered in the formulation. The new model can be incorporated into the conventional finite element analysis grid, in which several composite elements have fully grouted bolts embedded. In this way the mesh generation of large scale bolted rock structures becomes convenient and feasible. The model has been implemented in a FEM program, and a comparative study between the numerical analysis and a pull out field test has been carried out, from which the validity and the robustness of the new model are justified.

Keywords: Composite element, bolt, rock mass.

Notation/List of Symbols

$\{\Delta\delta\}_r$, $\{\Delta\delta\}_b$, $\{\Delta\delta\}_g$	nodal displacement increments assigned to the composite element corresponding to rock sub-element, bolt sub-element, grout sub-element, respectively
$\{\Delta u\}_g$, $\{\Delta u\}_g^c$, $\{\Delta u\}_g^p$	displacement increments of the grout segment g in the global coordinate system, local Cartesian coordinate system, local cylindrical coordinate system, respectively
$\{\Delta u\}_b$, $\{\Delta u\}_b^c$, $\{\Delta u\}_b^p$	displacement increments of the bolt segment b in the global coordinate system, local Cartesian coordinate system, local cylindrical coordinate system, respectively

$\{\Delta u\}^p_{rg}$, $\{\Delta u\}^p_{bg}$	relative displacement increments of rock-grout and bolt-grout interfaces in the local cylindrical coordinate system
$\{\Delta\varepsilon\}_r$, $\{\Delta\varepsilon\}^c_g$, $\{\Delta\varepsilon\}^c_b$	strain increments of the intact rock, grout, and bolt sub-elements, respectively
$\{\Delta\sigma\}_r$,$\{\Delta\sigma\}^c_g$, $\{\Delta\sigma\}^c_b$	stress increments of the intact rock, grout, and bolt sub-elements, respectively
[N]	shape function defined in composite element
$[B]_r$	strain matrix of rock sub-element
$[B]^c_g$, $[B]^c_b$	strain matrices of grout sub-element and bolt sub-element
$[l]^c$	displacement transformation matrix between the global and the local Cartesian coordinate systems
$[l]^p$	displacement transformation matrix between the Cartesian and cylindrical coordinate systems
ϕ, θ	dip direction and dip angle of the bolt segment
$[D]$, [S]	elastic matrix and elastic compliance matrix respectively
Δt	time stepping length
γ	fluidity parameter
F	yield function
Q	potential function
c_r, φ_r	cohesion and friction angle of intact rock
E, G, λ	Young's modulus, shear modulus, and Lamé coefficient, respectively
E_b, G_b	Young's modulus and shear modulus of bolt
σ_y, σ_u, γ_u^{vp}, γ^{vp}	yield strength, ultimate strength, ultimate plastic general shear strain, present plastic general shear strain of bolt, respectively
c_g, φ_g	cohesion and friction angle of grout
E_g, G_g	Young's modulus and shear modulus of grout
k_n, k_s	normal stiffness and tangential stiffness of interface
σ_T	tensile strength of interface
$\{\Delta\dot{\varepsilon}^{vp}\}_r$	viscoplastic flow rate of rock sub-element
$\{\Delta\dot{\varepsilon}^{vp}\}^c_b$, $\{\Delta\dot{\varepsilon}^{vp}\}^c_g$	viscoplastic flow rates of bolt sub-element and grout sub-element in the local Cartesian coordinate system
$\{\Delta\dot{\varepsilon}^{vp}\}^p_{bg}$, $\{\Delta\dot{\varepsilon}^{vp}\}^p_{rg}$	viscoplastic flow rates of bolt-grout interface sub-element and rock-grout interface sub-element in the local cylindrical coordinate system
$\{\Delta f\}_r$, $\{\Delta f\}_g$, $\{\Delta f\}_b$	nodal load increments in composite element transferred from rock sub-element, grout sub-element, bolt sub-element, respectively
$\{\Delta f^{vp}\}_r$, $\{\Delta f^{vp}\}_g$, $\{\Delta f^{vp}\}_b$, $\{\Delta f^{vp}\}_{rg}$, $\{\Delta f^{vp}\}_{bg}$	nodal load increments in composite element transferred from the viscoplastic strain increments of rock sub-element, grout sub-element, bolt sub-element, rock-grout interface sub-element, bolt-grout interface sub-element, respectively
$[k]_r$, $[k]_g$, $[k]_b$, $[k]_{rg}$, $[k]_{bg}$	stiffness matrices of rock sub-element, grout sub-element, bolt sub-element, rock-grout interface sub-element, bolt-grout interface sub-element, respectively

1. Introduction

Fully grouted rock bolts are widely used as a reinforcement in rock engineering. Laboratory and field tests have been conducted and a detailed understanding of the interaction between the rock bolts and the rock masses has been obtained (Hyett et al., 1992; Yazici and Kaiser, 1992; Kaiser et al., 1992; Bawden et al., 1992; Egger and

Pellet, 1991; Egger and Zabuski, 1991). Based on these semi-empirical formulae have been written on the one hand which are very useful in conventional design (St. John and Van Dillen, 1983; Spang and Egger, 1990). On the other hand, advanced numerical models have been developed, which can be classified into two categories: one is the explicit or distinct modeling of the bolts and the joints (Aydan, 1989; Swoboda and Marence, 1991; Swoboda and Marence, 1992; Chen and Egger, 1997), the other one is the equivalent modeling (Larsson and Olofsson, 1983; Larsson et al., 1985; Pande and Gerrard, 1983; Chen and Pande, 1994; Chen and Egger, 1999). Either of them has special advantages: the former has the potentiality to describe the bolt behaviour in every detail, and the latter can be applied to complicated engineering problems with a large number of joints and bolts.

Many researchers including the authors of this paper have been working in the area of equivalent modeling of fully bolted jointed rock masses, and some improvements have been made to describe the bolt behaviour more reasonably (e.g. the localized shear phenomenon at the joints). Laboratory tests and engineering applications have proved the value of such improvements (Chen and Egger, 1999). However, it should be recognized that so far some very complicated but important detailed phenomena (e.g. the pull out failure of the bolts) cannot be simulated satisfactorily by the equivalent approach. It is true that for very complicated engineering problems, a combination of both equivalent and explicit modeling is more feasible than only to make use of either one.

Aydan (1989) developed a three-dimensional bolt element with 8 nodal points. Two of these are connected to the bolt, whereas six others are connected to the rock mass. The number of nodes in the two-dimensional case is reduced to six. Swoboda and Marence (1991, 1992) modified Aydan's formulation, assigning different coordinates for the bolt nodes and the nodes of the rock-grout interfaces. Thus, the bolt and rock displacements are different at the bolt-joint intersection. In this way, the parameters in the stiffness matrix are not constant. They depend on the joint displacement and are independently calculated by an iterative procedure. Chen and Egger (1997) also developed a two dimensional explicit model of a bolt element with 6 nodes, of which two are connected to the bolt, whereas four others are connected to the rock mass, and a simplified analytical solution of the bolt deformation at the bolt-joint intersection is used.

All of the above explicit fully grouted bolt element models have the same characteristics: they are conventional elements which have definite nodes, and some of these nodes should be the common nodes of the nearby rock material elements. Consequently, the existence of a large quantity of bolts will impose very strong restraints on the finite element mesh generation, especially in three dimensional complicated structure problems. Naturally the question is put forward whether we can let the bolt elements be located inside conventional rock material elements.

The answer is positive by the composite element concept (Chen et al., 2003) which has been implemented in the case of hollow (or Swellex) rock bolts (Chen et al., 2002). What will be described in the following is the three dimensional formulation for the rock mass reinforced by fully grouted bolts. The bolt and grout are embedded within the element and treated separately, the interfaces between the bolt-grout material and the rock-grout material are taken into account, and the elasto-viscoplastic deformations are considered. The comparison study between the numerical analysis

and a pull out field test has been carried out, from which the validity and the robustness of the new model are justified.

2. Principle of the Composite Element Concept

2.1 The Concept of Composite Element and Sub-Element

Suppose a domain shown in Fig. 1 containing two sub-domains which have different mechanical characteristics. A composite element is defined to cover the whole domain. The sub-domains are defined as sub-elements which are not necessarily standard finite elements. The displacements $\{\Delta u\}_1$, $\{\Delta u\}_2$ in each sub-element are interpolated from the nodal displacements $\{\Delta\delta\}_1$, $\{\Delta\delta\}_2$ assigned to the composite element as (Fig. 1):

$$\{\Delta u\}_1 = [N]\{\Delta\delta\}_1 \quad \text{within the sub-element 1,} \tag{1}$$

$$\{\Delta u\}_2 = [N]\{\Delta\delta\}_2 \quad \text{within the sub-element 2.} \tag{2}$$

in which [N] is the shape function of the conventional FEM defined in the whole composite element. However, it should be pointed out that the interpolation expressed in Eqs. (1) and (2) is valid only in each of the sub-element respectively. The loads acting at each sub-element are transferred to the respective nodal values of the composite element as $\{\Delta f\}_1$, $\{\Delta f\}_2$, and the equilibrium equation can be established according to the virtual work principle as:

$$\begin{bmatrix} [k]_{11} & [k]_{12} \\ [k]_{21} & [k]_{22} \end{bmatrix} \begin{Bmatrix} \{\Delta\delta\}_1 \\ \{\Delta\delta\}_2 \end{Bmatrix} = \begin{Bmatrix} \{\Delta f\}_1 \\ \{\Delta f\}_2 \end{Bmatrix}. \tag{3}$$

With the solved nodal displacements $\{\Delta\delta\}_1$ and $\{\Delta\delta\}_2$, the displacements, the strains as well as the stresses in each sub-element can be calculated.

2.2 Special Consideration for the Rock Bolt

When the outline of the sub-element 1 is a conventional finite element, it can be used as a composite element, i.e. the composite element is the same as defined by the

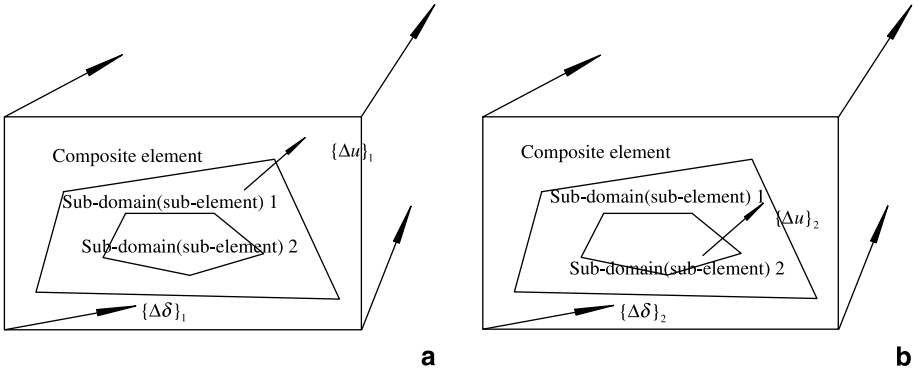

Fig. 1. The displacements interpolation in the composite element. **a** Displacement interpolation of sub-element 1, **b** displacement interpolation of sub-element 2

outline of the sub-element 1. In this way the composite element concept can be incorporated easily into the conventional finite element analysis procedure. This is just the case happening in the analysis of fully grouted rock bolts.

In the analysis of bolted rock structures with the composite model, the FE meshes can be generated without taking account of the existence of rock bolts. Then the dip directions and dip angles as well as the collar coordinates of the bolts will be put in. By simple calculations based on the geometry, the intersection conditions of each bolt with the FE grid can be obtained. Figure 2 shows a finite element which contains one bolt segment. As we have indicated above, this element can be defined as a composite element, within which there are five sub-elements representing: the rock material, the grout material, the bolt material, the rock-grout interface, and the bolt-grout interface respectively.

A global coordinate system is defined to formulate the overall governing equations, with the X-axis pointing Northward, the Y-axis pointing Westward, and the Z-axis being vertical. For each bolt a Cartesian local system is also needed to simplify the computation which is defined as follows (Fig. 3): the z_b-axis is along the bolt and upright, the y_b-axis is perpendicular to the bolt and points in the direction of dip and the x_b-axis is formed by the right hand rule. On the basis of the local Cartesian coordinate system the local cylindrical coordinate system is defined (Fig. 4). Let the subscripts r, g, b, rg, bg denote the quantities of the rock material, the grout material, the bolt, the interface between rock and grout, the interface between bolt

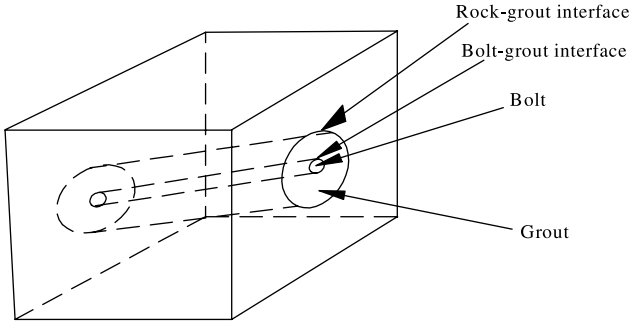

Fig. 2. Composite element containing five sub-elements

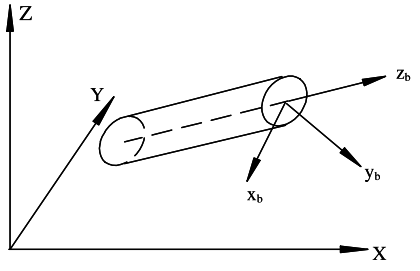

Fig. 3. Local coordinate system of the bolt (Cartesian)

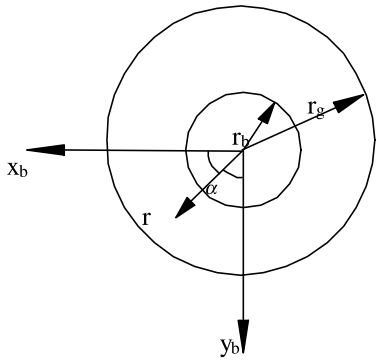

Fig. 4. Local coordinate system of the bolt (cylindrical)

and grout, respectively; the superscripts c and p are used to denote the quantities in the Cartesian and cylindrical local coordinate system.

The basic assumptions to be introduced for writing the governing equations are as follows:

a) At the cross section of the bolt or the grout, there are three stress increments: one normal stress (z_b direction) and two shear stresses (x_b and y_b directions);

b) At the interfaces between rock-grout and bolt-grout, there are three stress increments: one normal stress perpendicular to the interfaces (r direction) and two shear stresses along the interfaces (α and z directions).

2.3 Transformation Between the Different Coordinate Systems

For the bolt segment b, the displacement transformation between the global and the local coordinate systems is defined as follows:

$$\{\Delta u\}_b^c = [l]^c \{\Delta u\}_b. \tag{4}$$

The transforming matrix in Eq. (4) is:

$$[l]^c = \begin{bmatrix} -\sin\phi & \sin\theta\cos\phi & \cos\theta\cos\phi \\ -\cos\phi & -\sin\theta\sin\phi & -\cos\theta\sin\phi \\ 0 & -\cos\theta & \sin\theta \end{bmatrix}, \tag{5}$$

in which ϕ, θ are the dip direction and dip angle of the bolt segment respectively.

The displacement transformation between the Cartesian and cylindrical coordinate systems is defined as follows:

$$\{\Delta u\}_b^p = [l]^p \{\Delta u\}_b^c. \tag{6}$$

The transforming matrix in Eq. (6) is:

$$[l]^p = \begin{bmatrix} \cos\alpha & -\sin\alpha & 0 \\ \sin\alpha & \cos\alpha & 0 \\ 0 & 0 & 1 \end{bmatrix}, \tag{7}$$

in which the angle α is shown in Fig. 4.

For the grout material around the bolt the transformations are defined similarly:

$$\{\Delta u\}_g^c = [l]^c \{\Delta u\}_g \tag{8}$$

$$\{\Delta u\}_g^p = [l]^p \{\Delta u\}_g^c. \tag{9}$$

3. The Constitutive Equations of the Composite Element Containing Bolts

According to the elasto-viscoplastic potential theory (Owen and Hinton, 1980), at time t, the explicit constitutive equation will take the following forms:

$$\begin{cases} \{\Delta\sigma\} = [D](\{\Delta\varepsilon\} - \{\dot{\varepsilon}^{vp}\}\Delta t) \\ or \\ \{\Delta\varepsilon\} = [S]\{\Delta\sigma\} + \{\dot{\varepsilon}^{vp}\}\Delta t, \end{cases} \tag{10}$$

in which Δt is the time stepping length, [D] and [S] are the elastic matrix and compliance matrix respectively. The viscoplastic flow rate is:

$$\{\dot{\varepsilon}^{vp}\} = \gamma \prec F \succ \left\{ \frac{\partial Q}{\partial\{\sigma\}} \right\}, \tag{11}$$

in which γ is the fluidity parameter, F and Q are the yield and potential functions respectively, and the function $\langle \mathrm{F} \rangle$ is defined as:

$$\langle F \rangle = \begin{cases} F & if\ F > 0 \\ 0 & if\ F < 0. \end{cases} \tag{12}$$

If the fluidity parameter γ could be obtained then the histories as well as the steady-state results of the deformation and failure of a structure could be calculated. However, in some cases it is not easy to get the appropriate fluidity parameter or it is thought that only the elasto-plastic solution is of importance. Under such circumstances we can simply assume that the fluidity parameter $\gamma = 1$, in this way the histories are not applicable, but the steady-state results of deformation and failure are identical to the corresponding conventional static elasto-plastic solution.

3.1 The Constitutive Equation of Intact Rock

The rock material is taken as an isotropic material whose elastic matrix is:

$$[D]_r = \begin{bmatrix} \lambda + 2\mathrm{G} & \lambda & \lambda & 0 & 0 & 0 \\ & \lambda + 2\mathrm{G} & \lambda & 0 & 0 & 0 \\ & & \lambda + 2\mathrm{G} & 0 & 0 & 0 \\ & & & \mathrm{G} & 0 & 0 \\ & \mathrm{SYM} & & & \mathrm{G} & 0 \\ & & & & & \mathrm{G} \end{bmatrix}. \tag{13}$$

For the yield of the intact rock, both the Mohr-Coulomb and the Drucker-Prager criteria are widely used. In the present study the latter is implemented in a FEM program:

$$\begin{cases} F_r = aI_1 + \sqrt{J_2} - k = 0 \\ a = \sin\varphi_r / \sqrt{3(3 + \sin^2\varphi_r)} \\ k = \sqrt{3} c_r \cos\varphi_r / \sqrt{3 + \sin^2\varphi_r}. \end{cases} \tag{14}$$

The associated flow rule is adopted:

$$Q_r = F_r. \tag{15}$$

In Eqs. (14) c_r and φ_r are the cohesion and friction angle of the intact rock respectively.

3.2 The Constitutive Equation of the Bolt

The constitutive equation of the bolt is expressed in the local Cartesian coordinate system. According to the basic assumption (a), we have:

$$[D]_b^c = \begin{bmatrix} G_b & 0 & 0 \\ 0 & G_b & 0 \\ 0 & 0 & E_b \end{bmatrix}. \tag{16}$$

The von Mises criterion with linear work hardening is used for the bolt:

$$\begin{cases} F_b = [3(\tau_{bzx}^2 + \tau_{bzy}^2) + \sigma_b^2]^{1/2} - \sigma \\ \sigma = \sigma_y + (\sigma_u - \sigma_y)\gamma^{vp} / \gamma_u^{vp}, \end{cases} \tag{17}$$

in which σ_y, σ_u, γ_u^{vp}, γ^{vp} are the yield strength, ultimate strength, ultimate plastic general shear strain, and present plastic general shear strain respectively.

The associated flow rule is adopted.

3.3 The Constitutive Equation of Grout

Also the constitutive equation of the grout is expressed in the Cartesian local coordinate system. According to the basic assumption (a), we have:

$$[D]_g^c = \begin{bmatrix} G_g & 0 & 0 \\ 0 & G_g & 0 \\ 0 & 0 & E_g \end{bmatrix}, \tag{18}$$

the Drucker-Prager criterion is used for the yield of grout material:

$$\begin{aligned} F_g &= a\sigma_g + \sqrt{\frac{1}{3}}\sqrt{\sigma_g^2 + 3(\tau_{gzx}^2 + \tau_{gzy}^2)} - k = 0 \\ a &= \sin\varphi_g \Big/ \sqrt{3(3 + \sin^2\varphi_g)} \\ k &= \sqrt{3} c_g \cos\varphi_g \Big/ \sqrt{3 + \sin^2\varphi_g}, \end{aligned} \tag{19}$$

in which c_g and φ_g are cohesion and friction angle of grout material.

The associated flow rule is adopted:

$$Q_g = F_g. \tag{20}$$

3.4 The Constitutive Equation of Interfaces

The same relation is used for both the rock-grout interface and the bolt-grout interface. For simplicity the subscripts rg or bg are neglected in the following equations. According to the basic assumption (b), the elastic matrix of the interface in its local cylindrical coordinate system can be expressed by the normal stiffness k_n and the tangential stiffness k_s as:

$$[D]^p = \begin{bmatrix} k_s & 0 & 0 \\ 0 & k_n & 0 \\ 0 & 0 & k_s \end{bmatrix} \tag{21}$$

If a non-associated flow rule is considered for the interface, the yield function F and potential function Q are expressed by the cohesion c, friction angle φ, dilatancy angle ϕ and tensile strength σ_{T}:

$$\begin{cases} F = \sqrt{\tau_{r\alpha}^2 + \tau_{rz}^2} + \sigma_r tg\varphi - c, \quad if\ \sigma_r \prec \sigma_T \\ Q = \sqrt{\tau_{r\alpha}^2 + \tau_{rz}^2} + \sigma_r tg\phi + \text{const.} \end{cases} \tag{22}$$

$$\begin{cases} F = \sigma_r - \sigma_T, \quad if\ \sigma_r \geqslant \sigma_T \\ Q = \sqrt{\tau_{r\alpha}^2 + \tau_{rz}^2 + \sigma_r^2} + \text{const.} \end{cases} \tag{23}$$

It should be pointed out that in the case of the interfaces, the strain increment will be replaced by the relative displacement in the general form of the constitutive relation Eq. (10) which is denoted as:

$$\{\Delta u\}^p = \begin{Bmatrix} \Delta u_\alpha \\ \Delta u_r \\ \Delta u_z \end{Bmatrix}, \tag{24}$$

the corresponding stress increment at the interfaces is:

$$\{\Delta\sigma\}^p = \begin{Bmatrix} \Delta\tau_{r\alpha} \\ \Delta\sigma_r \\ \Delta\tau_{rz} \end{Bmatrix}. \tag{25}$$

4. The Equilibrium Equations of the Composite Element Containing Bolts

4.1 The Relationship Between the Strain Increment and the Nodal Displacement Increment

There are three sets of independent nodal displacement increments at the composite element e if there is one bolt segment. Each of them will be used to interpolate the displacement increments of the rock material, the grout material, and the bolt material

respectively:

$$\{\Delta u\}_r = [N]\{\Delta\delta\}_r, \tag{26}$$

$$\begin{cases} \{\Delta u\}_g^c = [N][L]^c\{\Delta\delta\}_g \\ \{\Delta u\}_g^p = [N][L]^p[L]^c\{\Delta\delta\}_g, \end{cases} \tag{27}$$

$$\begin{cases} \{\Delta u\}_b^c = [N][L]^c\{\Delta\delta\}_b \\ \{\Delta u\}_b^p = [N][L]^p[L]^c\{\Delta\delta\}_b. \end{cases} \tag{28}$$

The nodal displacement transformation matrices $[L]^c$ and $[L]^{\mathrm{p}}$ are defined by using the matrices $[l]^c$ and $[l]^{\mathrm{p}}$ in the Eqs. (4) to (7):

$$[L]^c = \begin{bmatrix} [l]^c & & & \\ & \cdot & & \\ & & \cdot & \\ & & & [l]^c \end{bmatrix}_{3n\times 3n} \tag{29}$$

$$[L]^p = \begin{bmatrix} [l]^p & & & \\ & \cdot & & \\ & & \cdot & \\ & & & [l]^p \end{bmatrix}_{3n\times 3n} \tag{30}$$

and the shape function matrix is given by the conventional finite element algorithm:

$$[N] = \begin{bmatrix} N_1 & 0 & 0 & N_2 & 0 & 0\cdots N_n & 0 & 0 \\ 0 & N_1 & 0 & 0 & N_2 & 0\cdots 0 & N_n & 0 \\ 0 & 0 & N_1 & 0 & 0 & N_2\cdots 0 & 0 & N_n \end{bmatrix}. \tag{31}$$

The strain increments of the intact rock, grout, and bolt materials are then calculated by:

$$\{\Delta\varepsilon\}_r = [B]_r\{\Delta\delta\}_r, \tag{32}$$

$$\{\Delta\varepsilon\}_g^c = [B]_g^c[L]^c\{\Delta\delta\}_g, \tag{33}$$

$$\{\Delta\varepsilon\}_b^c = [B]_b^c[L]^c\{\Delta\delta\}_b, \tag{34}$$

where

$$[B]_r = [[B]_{r1} \quad [B]_{r2} \quad \ldots [B]_{rn}], \tag{35}$$

$$[B]_g^c = \lfloor [B]_{g1}^c \quad [B]_{g2}^c \quad \ldots [B]_{gn}^c \rfloor, \tag{36}$$

$$[B]_b^c = \lfloor [B]_{b1}^c \quad [B]_{b2}^c \quad \ldots [B]_{bn}^c \rfloor, \tag{37}$$

$$[B]_{ri} = \begin{bmatrix} \frac{\partial N_i}{\partial X} & 0 & 0 \\ 0 & \frac{\partial N_i}{\partial Y} & 0 \\ 0 & 0 & \frac{\partial N_i}{\partial Z} \\ 0 & \frac{\partial N_i}{\partial Z} & \frac{\partial N_i}{\partial Y} \\ \frac{\partial N_i}{\partial Z} & 0 & \frac{\partial N_i}{\partial X} \\ \frac{\partial N_i}{\partial Y} & \frac{\partial N_i}{\partial X} & 0 \end{bmatrix}, \tag{38}$$

$$[B]_{gi}^{c} = \begin{bmatrix} \frac{\partial N_i}{\partial z_g^c} & 0 & \frac{\partial N_i}{\partial x_g^c} \\ 0 & \frac{\partial N_i}{\partial z_g^c} & \frac{\partial N_i}{\partial y_g^c} \\ 0 & 0 & \frac{\partial N_i}{\partial z_g^c} \end{bmatrix}, \tag{39}$$

$$[B]_{bi}^{c} = \begin{bmatrix} \frac{\partial N_i}{\partial z_b^c} & 0 & \frac{\partial N_i}{\partial x_b^c} \\ 0 & \frac{\partial N_i}{\partial z_b^c} & \frac{\partial N_i}{\partial y_b^c} \\ 0 & 0 & \frac{\partial N_i}{\partial z_b^c} \end{bmatrix}. \tag{40}$$

The displacement increments in the rock, grout, and bolt materials will cause relative displacement increments at the rock-grout and the bolt-grout interfaces. These increments will be expressed in the local cylindrical coordinate system:

$$\{\Delta u\}_{rg}^{p} = \{\Delta u\}_{r}^{p} - \{\Delta u\}_{g}^{p} = [N][L]^{p}[L]^{c}(\{\Delta\delta\}_{r} - \{\Delta\delta\}_{g}), \tag{41}$$

$$\{\Delta u\}_{bg}^{p} = \{\Delta u\}_{g}^{p} - \{\Delta u\}_{b}^{p} = [N][L]^{p}[L]^{c}(\{\Delta\delta\}_{g} - \{\Delta\delta\}_{b}). \tag{42}$$

4.2 The Equilibrium Equation Expressed by the Nodal Displacement and Load Increments

Suppose virtual displacements occur for intact rock material, grout material, and bolt material as:

$$(\{\Delta u\}_{r})^{*} = [N](\{\Delta\delta\}_{r})^{*}, \tag{43}$$

$$(\{\Delta u\}_{g}^{c})^{*} = [N][L]^{c}(\{\Delta\delta\}_{g})^{*}, \tag{44}$$

$$(\{\Delta u\}_{b}^{c})^{*} = [N][L]^{c}(\{\Delta\delta\}_{b})^{*}. \tag{45}$$

The corresponding virtual strains and relative displacements will be:

$$(\{\Delta\varepsilon\}_{r})^{*} = [B]_{r}(\{\Delta\delta\}_{r})^{*}, \tag{46}$$

$$(\{\Delta\varepsilon\}_{g}^{c})^{*} = [B]_{g}^{c}[L]^{c}(\{\Delta\delta\}_{g})^{*}, \tag{47}$$

$$(\{\Delta\varepsilon\}_{b}^{c})^{*} = [B]_{b}^{c}[L]^{c}(\{\Delta\delta\}_{b})^{*}, \tag{48}$$

$$(\{\Delta u\}_{rg}^{p})^{*} = [N][L]^{p}[L]^{c}((\{\Delta\delta\}_{r})^{*} - (\{\Delta\delta\}_{g})^{*}), \tag{49}$$

$$(\{\Delta u\}_{bg}^{p})^{*} = [N][L]^{p}[L]^{c}((\{\Delta\delta\}_{g})^{*} - (\{\Delta\delta\}_{b})^{*}). \tag{50}$$

The virtual work principle for the composite element will be written in the following form:

$$W_r + W_g + W_b + W_{rg} + W_{bg} = (\{\Delta\delta\}_{r})^{*T}\{\Delta f\}_{r} + (\{\Delta\delta\}_{g})^{*T}\{\Delta f\}_{g} + (\{\Delta\delta\}_{b})^{*T}\{\Delta f\}_{b}, \tag{51}$$

where $\{\Delta f\}_{r}$, $\{\Delta f\}_{g}$, $\{\Delta f\}_{b}$ are the nodal load increments at the composite element, which can be transferred from the load increments acting at the rock, grout, and bolt

materials according to the same algorithm as in the conventional finite element method.

4.2.1 The Virtual Work Contributed from the Rock Material

$$W_r = \int_{\Omega_r} (\{\Delta\varepsilon\}_r)^{*T} \{\Delta\sigma\}_r d\Omega$$

By taking the constitutive relation Eq. (10) and the strain-displacement relation Eq. (32) into account, the virtual work in the rock material becomes:

$$W_r = \int_{\Omega_r} (\{\Delta\delta\}_r)^{*T} [B]_r^T [D]_r ([B]_r \{\Delta\delta\}_r - \{\dot{\varepsilon}^{vp}\}_r \Delta t) d\Omega. \tag{52}$$

4.2.2 The Virtual Work Contributed from the Grout Material

$$W_g = \int_{\Omega_g} (\{\Delta\varepsilon\}_g^c)^{*T} \{\Delta\sigma\}_g^c d\Omega$$

By inserting the constitutive relation Eq. (10) and the strain-displacement relation Eq. (33) into the above expression, the virtual work in the grout material will be:

$$W_g = \int_{\Omega_g} (\{\Delta\delta\}_g)^{*T} [L]^{cT} [B]_g^{cT} [D]_g^c ([B]_g^c [L]^c \{\Delta\delta\}_g - \{\dot{\varepsilon}^{vp}\}_g^c \Delta t) d\Omega. \tag{53}$$

4.2.3 The Virtual Work Contributed from the Bolt Material

In a similar way as for the grout material, the virtual work in the bolt material is:

$$W_b = \int_{\Omega_b} (\{\Delta\delta\}_b)^{*T} [L]^{cT} [B]_b^{cT} [D]_b^c ([B]_b^c [L]^c \{\Delta\delta\}_b - \{\dot{\varepsilon}^{vp}\}_b^c \Delta t) d\Omega. \tag{54}$$

4.2.4 The Virtual Work Contributed from the Rock-Grout Interface

$$W_{rg} = \int_{S_{rg}} (\{\Delta u\}_{rg}^p)^{*T} \{\Delta\sigma\}_{rg}^p dS$$

By introducing the constitutive relation Eq. (10) and the strain-displacement relation Eq. (41) into W_{rg}, the following can be derived:

$$\begin{aligned} W_{rg} = \int_{S_{rg}} (&(\{\Delta\delta\}_r)^{*T} \\ &- (\{\Delta\delta\}_g)^{*T}) [L]^{cT} [L]^{pT} [N]^T [D]_{rg}^p ([N][L]^p [L]^c (\{\Delta\delta\}_r - \{\Delta\delta\}_g) \\ &- \{\dot{\varepsilon}^{vp}\}_{rg}^p \Delta t) dS. \end{aligned} \tag{55}$$

4.2.5 The Virtual Work Contributed from the Bolt-Grout Interface

As for the rock-grout interface, the virtual work in the bolt-grout interface can be written directly:

$$W_{bg} = \int_{S_{bg}} (\{\Delta\delta\}_g)^{*T} - (\{\Delta\delta\}_b)^{*T})[L]^{cT}[L]^{p}[N]^{T}[D]^{p}_{bg}([N][L]^{p}[L]^{c}(\{\Delta\delta\}_g - \{\Delta\delta\}_b) - \{\dot{\varepsilon}^{vp}\}^{p}_{bg}\Delta t)dS. \tag{56}$$

Now introduce Eqs. (52) to (56) into Eq. (51) and arrange the equation according to the different virtual displacements of the rock material, the grout material, and the bolt material. Noting that the virtual displacements $(\{\Delta\delta\}_r)^*$, $(\{\Delta\delta\}_g)^*$, $(\{\Delta\delta\}_b)^*$ are arbitrary vectors, the validity of the virtual work principle will lead to the following equations:

$$\begin{cases} ([k]_r + [k]_{rg})\{\Delta\delta\}_r - [k]_{rg}\{\Delta\delta\}_g = \{\Delta f\}_r + \{\Delta f^{vp}\}_r + \{\Delta f^{vp}\}_{rg} \\ -[k]_{rg}\{\Delta\delta\}_r + ([k]_g + [k]_{rg} + [k]_{bg})\{\Delta\delta\}_g - [k]_{bg}\{\Delta\delta\}_b = \{\Delta f\}_g + \{\Delta f^{vp}\}_g - \{\Delta f^{vp}\}_{rg} + \{\Delta f^{vp}\}_{bg} \\ -[k]_{bg}\{\Delta\delta\}_g + ([k]_b + [k]_{bg})\{\Delta\delta\}_b = \{\Delta f\}_b + \{\Delta f^{vp}\}_b - \{\Delta f^{vp}\}_{bg}, \end{cases} \tag{57}$$

in which:

$$\begin{cases} [k]_r = \int_{\Omega_r}[B]^T_r[D]_r[B]_r d\Omega \\ [k]_g = \int_{\Omega_g}[L]^{cT}[B]^T_g[D]^c_g[B]_g[L]^c d\Omega \\ [k]_b = \int_{\Omega_b}[L]^{cT}[B]^T_b[D]^c_b[B]_b[L]^c d\Omega \\ [k]_{rg} = \int_{S_{rg}}[L]^{cT}[L]^{pT}[N]^T[D]^p_{rg}[N][L]^p[L]^c dS \\ [k]_{bg} = \int_{S_{bg}}[L]^{cT}[L]^{pT}[N]^T[D]^p_{bg}[N][L]^p[L]^c dS, \end{cases} \tag{58}$$

$$\begin{cases} \{\Delta f^{vp}\}_r = \int_{\Omega_r}[B]^T_r[D]_r\{\dot{\varepsilon}^{vp}\}_r\Delta t d\Omega \\ \{\Delta f^{vp}\}_g = \int_{\Omega_g}[L]^{cT}[B]^{cT}_g[D]^c_g\{\dot{\varepsilon}^{vp}\}^c_g\Delta t d\Omega \\ \{\Delta f^{vp}\}_b = \int_{\Omega_b}[L]^{cT}[B]^{cT}_b[D]^c_b\{\dot{\varepsilon}^{vp}\}^c_b\Delta t d\Omega \\ \{\Delta f^{vp}\}_{rg} = \int_{S_{rg}}[L]^{cT}[L]^{pT}[N]^T[D]^p_{rg}\{\dot{\varepsilon}^{vp}\}^p_{rg}\Delta t dS \\ \{\Delta f^{vp}\}_{bg} = \int_{S_{bg}}[L]^{cT}[L]^{pT}[N]^T[D]^p_{bg}\{\dot{\varepsilon}^{vp}\}^p_{bg}\Delta t dS. \end{cases} \tag{59}$$

5. Numerical Example

The model described in this paper has been implemented in the finite element code CORE3 which already allows for the equivalent modeling of reinforced jointed rock masses (Chen and Egger, 1999).

5.1 Calculation Conditions

A series of rock block samples of 5 m × 5 m × 6 m (length × width × height) has been studied. In the centre of the rock block a fully-grouted bolt (Fig. 5) is subjected to a

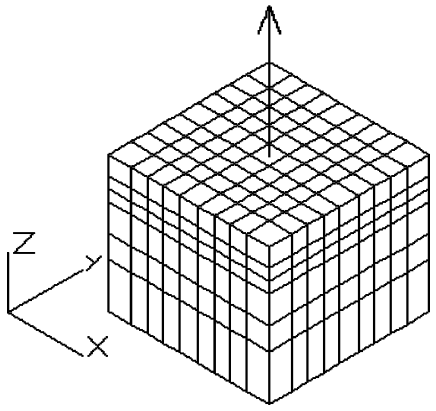

Fig. 5. Three dimensional FE mesh of the test sample

pull out force acting at the top face. The bottom of the block is fixed and the four vertical edge planes are free in the calculation. The length of the bolt is 3 m, the radii of bolt and grout are 20 mm and 38 mm respectively. The pull out loads are increased by 3 steps in the test: 300 kN, 600 kN, 720 kN. The experimental data used as reference data were obtained in the field test conducted at the excavated rock slope of the ship lock in the Three Gorges Project, China (Rong et al., 2001). The rock block samples are classified into several groups according to the characteristics of the rock masses. In this paper the comparative study between numerical analysis and field test will be conducted with a test group including two samples. During the experiment the axial stresses along the bolts and the displacements of the borehole collar are measured. Unfortunately, there are no data about the shear stresses and the displacements along the whole bolts.

Table 1. Material parameters

Material	E [GPa]	ν	c [MPa]	ϕ [°]	σ_T [MPa]	σ_y [MPa]	σ_u [MPa]	γ_u^{vp}
Steel	200	0.25				310	500	0.18
Grout	26	0.17	2.5	58	1.1			
Rock	32	0.2	1.7	59	1.1			

Table 2. Interface parameters

Material	K_n [MN/m^3]	K_s [MN/m^3]	c [MPa]	φ [°]	ϕ [°]	σ_T [MPa]
Rock-grout	10 000	2000	1	50	50	1
Bolt-grout	10 000	3000	2	58	58	1

5.2 Results

Figures 6 to 8 present a comparison between the experimental results and the computational results using the composite element model implemented in this paper. The experimental results show, as common in field tests in rock engineering, a large scatter. However, if the parameters can be selected properly, the computation shows to yield reasonable results. It is found that the computed axial displacements of the borehole collar are larger than the values measured in the tests (Fig. 8). A possible reason for this is that the Young's modulus of the rock and the stiffness values of the interfaces between the rock and the grout or between the grout and the bolt are underestimated.

Figures 9 to 15 show a set of computational results (no test results are available) which give a general view of the displacements of the bolt, grout and rock block as well as the shear stresses at the interfaces. It is interesting to point out that near the

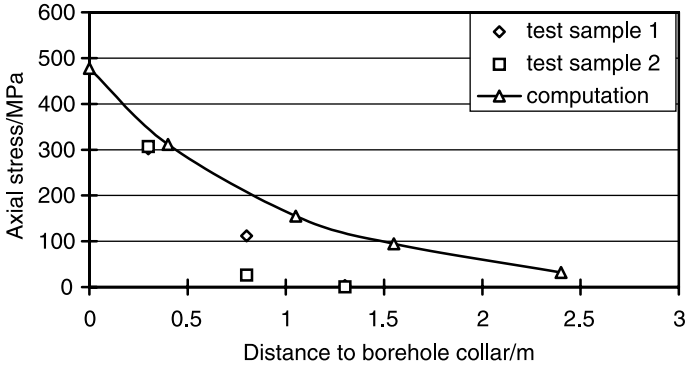

Fig. 6. Axial stress distribution along the bolt under 600 kN pull out force

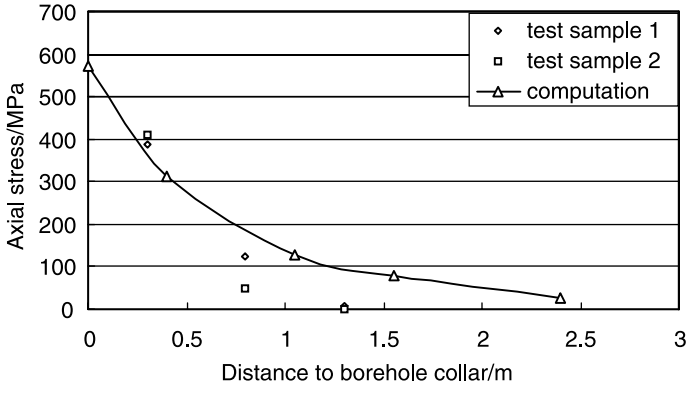

Fig. 7. Axial stress distribution along the bolt under 720 kN pull out force

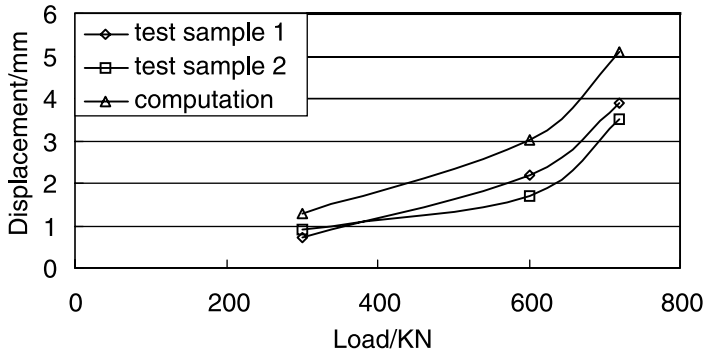

Fig. 8. Axial displacements of the borehole collar

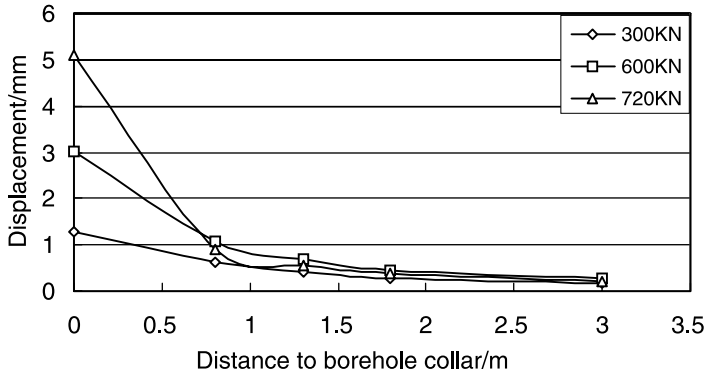

Fig. 9. Axial displacement distribution along the bolt

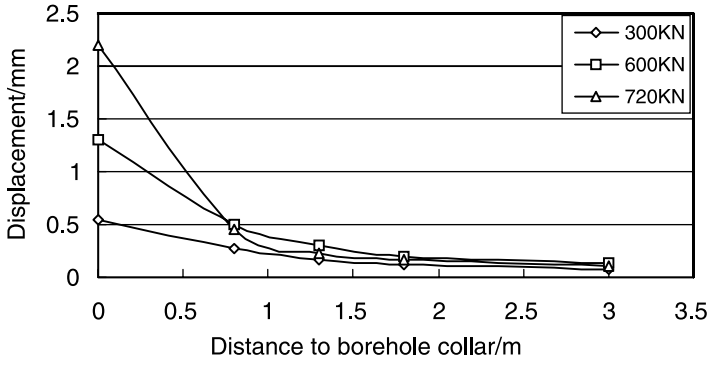

Fig. 10. Axial displacement distribution along the grout

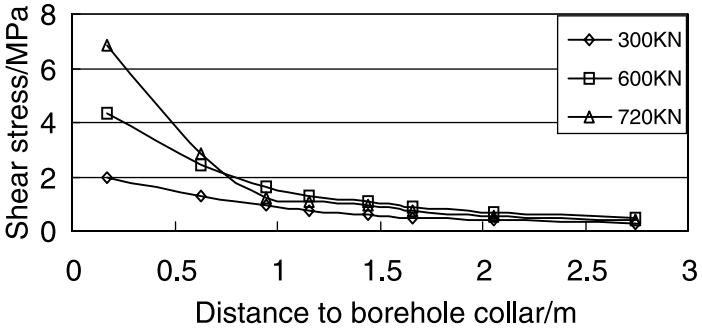

Fig. 11. Shear stress distribution along the interface between bolt and grout

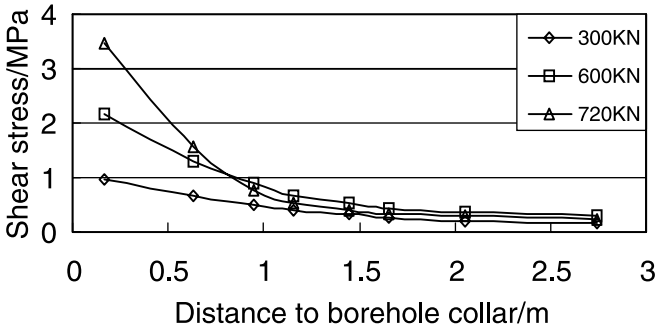

Fig. 12. Shear stress distribution along the interface between rock and grout

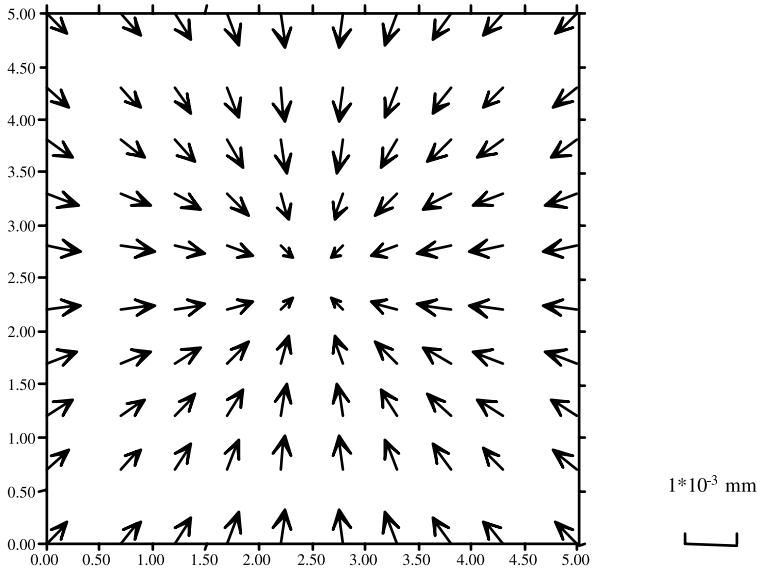

Fig. 13. Displacement vector of rock on the horizontal section (X–Y) of the test block at the elevation of Z = 4.2 m under 600 kN pull out force

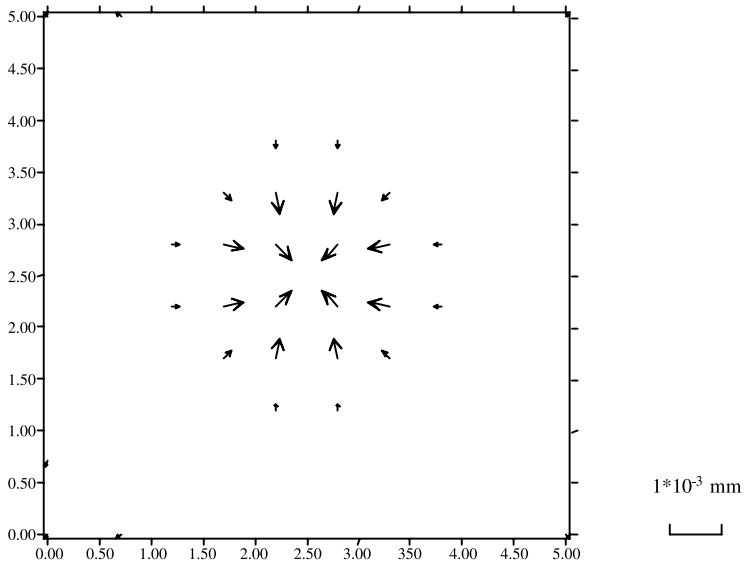

Fig. 14. Displacement vector of rock on the horizontal section (X–Y) of the test block at the elevation of Z = 5.2 m under 600 kN pull out force

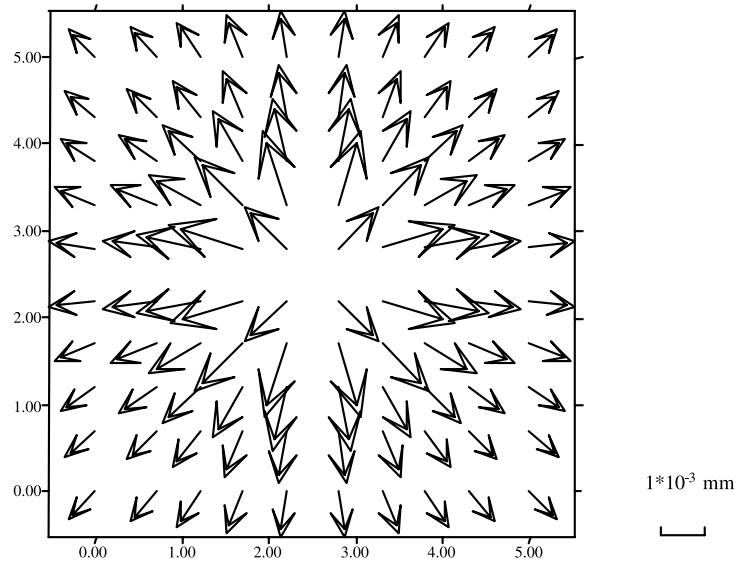

Fig. 15. Displacement vector of rock on the horizontal section (X–Y) of the test block at the elevation of Z = 6.0 m under 600 kN pull out force

borehole collar the displacements of the rock block have a tendency away from the bolt, while at a certain depth under the collar the displacements of the rock block are concentrated towards the bolt (Figs. 13 to 15).

It is worthwhile to point out that the above results are generally in accordance with the theoretical studies of bolt pull out tests (Farmer, 1975): the axial stress and the displacement of the bolt decrease exponentially from the point of loading to the far end of the bolt before a decoupling of the interfaces occurs.

6. Conclusions

The research presented in this paper is based on a new concept of ''composite element''. In such an element some sub-domains of any shape called sub-elements are contained. For each sub-element there are mapped displacements at the composite element nodes. The displacements, strains, and stresses within the sub-elements are calculated by the corresponding mapped nodal displacements of the composite element. The mapped sub-element displacements in the composite element can be solved by procedures similar to those used in the conventional finite element method. In the case when the outline of a sub-domain which contains all of the other sub-domains is the same as a conventional finite element, then it can be used as a composite element directly. In this way the composite elements can be easily integrated into the conventional finite elements system. The explicit fully grouted rock bolt element model presented in this paper has been described as a special example of the implementation of the method.

It is clear that in presence of a rock bolt, the degrees of freedom of displacement of the composite element will be tripled compared to those in the conventional finite element. These degrees of freedom come from the rock material, the grout material and the bolt material respectively. The rock-grout and bolt-grout interfaces have no independent degrees of freedom of displacement, the relative displacements and the stresses at the interfaces depend on the displacements of the rock, grout and bolt materials. In this way these materials are correlated, and the slip deformation and failure phenomena can be simulated.

Field tests carried out on fully grouted rock bolt confirm the correctness of the new model proposed. However, the new model should be further improved in order to describe the local behaviour of the bolt along the joints.

Acknowledgements

The work is supported by the Natural Science Foundation of China (50239070). The support of the national key laboratory of water resources and hydropower engineering (Wuhan University, China) is also appreciated.

References

Aydan, O. (1989): The stabilisation of rock engineering structures by rockbolts. Ph.D Thesis, Nagoya University, Japan.

Chen, S. H., Egger, P. (1997): Elasto-viscoplastic distinct modelling of bolts in jointed rock masses. In: Proc., 9th Int. Conf. on Computer Meth. and Advances in Geomech., Wuhan, P.R. China, 1985–1990.

Chen, S. H., Egger, P. (1999): Three dimensional elasto-viscoplastic finite element analysis of reinforced rock masses and its application. Int. J. Numer. Anal. Methods Geomech. 3(1), 61–78.

Chen, S. H., Pande, G. N. (1994): Rheological model and finite element analysis of jointed rock masses reinforced by passive, fully-grouted bolts. Int. J. Rock Mech. Min. Sci. Geomech. Abstr. 31(3), 273–277.

Chen, S. H., Qiang, S., Chen, S. F. (2003): Study on the three-dimensional composite element model of bolted rock masses. Chin. J. Rock Mech. Engng. 22(1), 1–8.

Chen, S. H., Egger, P., Migliazza, R., Giani, G. P. (2002): Three dimensional composite modelling of hollow bolts in rock masses. In: Proc., ISRM Int. Symp. on Rock Eng. for Mountainous Regions – Eurock'2002, Madeira, Portugal.

Egger, P., Pellet, F. (1991): Strength and deformation properties of reinforced jointed media under true triaxial conditions. In: Proc., 7th ISRM Cong., Aachen, Germany, 215–220.

Egger, P., Zabuski, L. (1991): Behaviour of rough bolted joints in direct shear tests. In: Proc., 7th ISRM Cong., Aachen, Germany, 1285–1288.

Farmer, I. W. (1975): Stress distribution along a resin grouted rock anchor. Int. J. Rock Mech. Min. Sci. Geomech. Abstr. 12, 347–351.

Hyett, A. J. et al. (1992): The effect of rock mass confinement and the bond strength of fully grouted cable bolts. Int. J. Rock Mech. Min. Sci. Geomech. Abstr. 29(5), 503–524.

Kaiser, P. K. et al. (1992): Effect of stress change on the bond strength of fully grouted cables. Int. J. Rock Mech. Min. Sci. Geomech. Abstr. 29(3), 293–306.

Larsson, H., Olofsson, T. (1983): Bolt action in jointed rock. In: Proc., Int. Symp. on Rock Bolting, Abisko, Sweden, 33–46.

Larsson, H., Olofsson, T., Stephansson, O. (1985): Reinforcement of jointed rock mass – a non linear continuum approach. In: Proc., Int. Symp. on Fundamentals of Rock Joints, Bjorkliden, Sweden, 567–577.

Owen, D. R. J., Hinton, E. (1980): Finite elements in plasticity: theory and practice. Pineridge Press Ltd., Swansea, U.K.

Pande, G. N., Gerrard, C. M. (1983): The behaviour of reinforced jointed rock masses under various simple loading states. In: Proc., 5th ISRM Cong., Melbourne, Australia, F217–F223.

Rong, G., Zhu, H. C., Yang, S. L. (2001): Field test of rock bolt in the Three Gorges Project ship lock slope. Rock Soil Mech. 22(2), 171–175.

St. John, C. M., Van Dillen, D. E. (1983): Rockbolts: A new representation and its application in tunnel design. In: Proc., 24th U.S. Symp. on Rock Mechanics, 13–25.

Spang, K., Egger, P. (1990): Action of fully-grouted bolts in jointed rock and factors of influence. Rock Mech. Rock Engng. 23(1), 201–229.

Swoboda, G., Marence, M. (1991): FEM modelling of rockbolts. In: Proc., Comp. Meth. and Adv. in Geomech., Cairns, Australia, 1515–1520.

Swoboda, G., Marence, M. (1992): Numerical modelling of rock bolts in intersection with fault system. In: Proc., Numerical Models in Geomechanics, NUMOG 5, Swansea, U.K., 729–738.

Yazici, S., Kaiser, P. K. (1992): Bond strength of grouted cable bolts. Int. J. Rock Mech. Min. Sci. 29(3), 279–292.

Authors' address: Prof. Chen Sheng-hong, Department of Hydroelectrical Engineering, Wuhan University, Wuhan, Hubei, 430072, P.R. China; e-mail: shchen@wuhee.edu.cn